

Multi-mode Transmission for the MIMO Broadcast Channel with Imperfect Channel State Information

Jun Zhang, Marios Kountouris, Jeffrey G. Andrews, and Robert W. Heath Jr.

Abstract

This paper proposes an adaptive multi-mode transmission strategy to improve the spectral efficiency achieved in the multiple-input multiple-output (MIMO) broadcast channel with delayed and quantized channel state information. The adaptive strategy adjusts the number of active users, denoted as the *transmission mode*, to balance transmit array gain, spatial division multiplexing gain, and residual inter-user interference. Accurate closed-form approximations are derived for the achievable rates for different modes, which help identify the active mode that maximizes the average sum throughput for given feedback delay and channel quantization error. The proposed transmission strategy is combined with round-robin scheduling, and is shown to provide throughput gain over single-user MIMO at moderate signal-to-noise ratio. It only requires feedback of instantaneous channel state information from a small number of users. With a feedback load constraint, the proposed algorithm provides performance close to that achieved by opportunistic scheduling with instantaneous feedback from a large number of users.

Index Terms

MIMO systems, space division multiplexing, broadcast channels, feedback, delay effects.

I. INTRODUCTION

Multi-user MIMO (MU-MIMO), which allows the base station (BS) to communicate with multiple mobile users simultaneously, provides spatial division multiplexing gain¹ proportional

J. Zhang, J. G. Andrews, and R. W. Heath Jr. are with the Wireless Networking and Communications Group, Department of Electrical and Computer Engineering, The University of Texas at Austin (Email: jzhang06@mail.utexas.edu, {jandrews, rheath}@ece.utexas.edu). M. Kountouris is with SUPELEC, France (Email: marios.kountouris@supelec.fr). This work has been supported in part by AT&T Labs, Inc. A conference version appeared in *Proc. IEEE Int. Symp. Information Theory 2009*. Last updated: October 24, 2018.

¹In this paper, we use the *spatial division multiplexing gain* to denote the spatial multiplexing gain provided by MU-MIMO to differentiate it from that provided by the point-to-point MIMO.

to the number of antennas (N_t) at the BS even with single-antenna mobiles [1], i.e. the sum throughput grows linearly with N_t at high SNR. To exploit the full spatial division multiplexing gain in the MIMO broadcast channel (MIMO-BC), channel state information at the transmitter (CSIT) is required to separate the spatial channels for different users. CSIT, however, is difficult to obtain and is never perfect. Imperfect CSIT causes residual inter-user interference, which degrades the performance of the MIMO-BC [2]. The capacity region of the MIMO-BC with imperfect CSIT has not been fully discovered. Although not capacity achieving, linear precoding is a practical transmission technique for the MIMO-BC; it is able to provide full spatial division multiplexing gain given CSIT [3], [4].

Limited feedback, in which users feed back quantized channel information through a feedback channel, is an efficient way to provide partial CSIT for the MIMO-BC [5]. It has been shown that the full spatial division multiplexing gain in the MIMO-BC can be obtained with carefully designed feedback strategies and a feedback rate that grows linearly with SNR (in dB) and the number of transmit antennas [6]–[9]. Therefore, linear precoding combined with limited feedback provides a feasible way to exploit the spatial division multiplexing gain in the MIMO-BC.

A. Related Work

In existing commercial wireless communication systems, the number of feedback bits for each user is fixed and cannot be adjusted with SNR. In addition, there are other CSIT imperfections, such as estimation error and feedback delay, all of which make the system throughput-limited at high SNR due to the residual inter-user interference [6], [9]. One approach to improve the CSIT accuracy in limited feedback systems is to employ multiuser diversity, as proposed in [7]. To reduce feedback overhead in such systems, threshold based feedback can be adopted [10]. The CSIT accuracy of limited feedback can also be improved with a progressive refinement of precoding vectors by taking advantage of the temporal channel coherence [11]. An alternative approach to deal with imperfect CSIT is adaptively switching between the single-user (SU) and multi-user (MU) modes², as the SU mode does not suffer from residual interference at high SNR. SU/MU mode switching algorithms for the random orthogonal beamforming system were proposed in [14], [15], where each user feeds back its preferred mode and the channel quality information (CQI). For the MIMO downlink with the number of receive antennas greater than or equal to the number of transmit antennas, an adaptive SU/MU mode switching algorithm was proposed in [16], which also considered correlation at transmit antennas.

²Note that the term “mode” used in this paper denotes the number of active users rather than different MIMO transmission techniques, as spatial multiplexing/diversity mode [12], or different number of data streams for a given user, as in [13].

Most prior mode switching algorithms were based on instantaneous CSIT; no explicit *mode switching point* has been obtained that is related to the key system parameters. An alternative approach is to switch based on the channel distribution information. In [17], the number of active users for a limited-feedback zero-forcing (ZF) precoding system was optimized through asymptotic analysis to maximize the spectral efficiency, based on average SNR and channel quantization codebook size. In [18], a SU/MU mode switching algorithm was proposed for the ZF precoding system considering delayed and quantized CSIT. The mode switching point can be explicitly derived based on the parameters including average SNR, normalized Doppler frequency, and codebook size, which are computable at the BS.

Both switching algorithms in [17] and [18] require only the selected users to feed back their instantaneous channel information, which is desirable for systems with a large number of users. The technique in [18] is based on non-asymptotic analysis, and thus can better characterize the system behavior with different system parameters, e.g. the operating regions for both SU and MU modes can be determined for different delay/mobility or different codebook sizes. However, it only switches between the SU mode and the MU mode serving as many users as transmit antennas. It neglects the impact of the number of active users on transmit array gain, spatial division multiplexing gain, and residual inter-user interference.

B. Contributions

In this paper, we propose a general multi-mode switching algorithm that adaptively selects the number of active users in a MIMO-BC considering delayed and quantized CSIT. We derive accurate closed-form approximations for the achievable rates for different modes, based on which the mode that provides the highest throughput can be selected. Such multi-mode transmission (MMT) strategy improves the spectral efficiency by balancing transmit array gain, spatial division multiplexing gain, and residual interference.

The proposed MMT strategy can be combined with channel-independent scheduling algorithms, such as round-robin scheduling, to serve a large number of users. In this way, the scheduling is of low complexity, and it greatly reduces the amount of feedback as only the pre-selected users need to feed back their instantaneous channel information for the precoder design. As instantaneous CSIT is not exploited, the proposed algorithm cannot provide multiuser diversity gain, but it is still able to provide a throughput gain over SU-MIMO transmission and can serve multiple users simultaneously. In addition, in certain scenarios such as with a feedback overhead constraint it is able to provide performance close to that achieved by opportunistic scheduling based on instantaneous CSI feedback from a large number of users.

Based on analytical and numerical results, we provide the following insights and guidelines for the design of MIMO transmission in the broadcast channel with imperfect CSIT:

- 1) The SU mode should be applied at both low and high SNRs; at medium SNR, the MU mode can be used with the number of active users adaptively adjusted. The full MU mode that serves N_t users normally should not be activated, as it has the highest residual interference and no array gain.
- 2) For practical systems such as 3GPP LTE, the MU mode should only be used with low mobility and the number of feedback bits should be increased or advanced feedback techniques such as progressive refinement [11] should be employed. A short frame length is desirable for MU-MIMO, as it is related to the amount of CSIT delay.
- 3) Considering delay-mobility and channel quantization, our analysis can determine which source dominates the CSIT imperfection. For given delay-mobility, we should provide a sufficiently large codebook size, as otherwise channel quantization error will dominate the performance; on the other hand, there is no need for a too large codebook size, as other CSIT imperfections such as delay-mobility start to dominate the performance.
- 4) For a fixed transmission mode, MMSE precoding outperforms ZF precoding. With imperfect CSIT, both precoding schemes require multi-mode transmission to improve the achievable rate, and they provide close performance. As ZF precoding with MMT requires less feedback and its preferred mode can be easily calculated, it is preferred to MMSE precoding.
- 5) If there is a constraint on the total number of feedback bits, high-quality feedback from less than N_t users together with mode selection provides good performance compared to instantaneous feedback from a large number of users.

Compared to our previous study in [18], this paper has made important extensions. First, we have explicitly considered the impact of the number of active users on the performance of MU-MIMO, while [18] only considered the full MU mode with N_t users. Second, the proposed MMT strategy can be easily extended to serve a large number of users and provide a significant throughput gain, while the dual-mode switching in [18] is inflexible and is confined in a system with N_t users. Third, the analysis and simulation results in this paper provide useful insights for the practical system design, while [18] emphasized analysis.

Organization: The rest of the paper is organized as follows: the system model and some assumptions are presented in Section II. In Section III, closed-form approximations are derived for the average achievable rates for different modes. User scheduling based on MMT is proposed in Section IV. Numerical results and conclusions are in Section V and VI, respectively.

Notation: In this paper, we use uppercase boldface letters for matrices (\mathbf{X}) and lowercase boldface for vectors (\mathbf{x}). $\mathbb{E}[\cdot]$ is the expectation operator. The conjugate transpose of a matrix \mathbf{X} (vector \mathbf{x}) is \mathbf{X}^* (\mathbf{x}^*). Similarly, \mathbf{X}^\dagger denotes the pseudo-inverse, $\tilde{\mathbf{x}}$ denotes the normalized vector of \mathbf{x} , i.e. $\tilde{\mathbf{x}} = \frac{\mathbf{x}}{\|\mathbf{x}\|}$, and $\hat{\mathbf{x}}$ denotes the quantized vector of $\tilde{\mathbf{x}}$.

II. SYSTEM MODEL

We consider a MIMO-BC with N_t antennas at the transmitter and U single-antenna mobiles. The discrete-time complex baseband received signal at the u -th user at time n is given as

$$y_u[n] = \mathbf{h}_u^*[n] \sum_{v=1}^M \mathbf{f}_v[n] x_v[n] + z_u[n], \quad (1)$$

where M is the active mode, i.e. the number of active users, $M = 1, 2, \dots, N_t$, $\mathbf{h}_u[n]$ is the channel vector for the u -th user, $\mathbf{h}_u[n] \in \mathbb{C}^{(N_t \times 1)}$, and $z_u[n]$ is normalized complex additive Gaussian noise, $z_u[n] \sim \mathcal{CN}(0, 1)$. $x_u[n]$ and $\mathbf{f}_u[n]$ are the transmit signal and precoding vector for the u -th user, and $\mathbf{f}_u[n] \in \mathbb{C}^{(N_t \times 1)}$. The transmit power constraint is $\mathbb{E} \left[\sum_{u=1}^M |x_u[n]|^2 \right] = P$, and we assume equal power allocation among different users. As the noise is normalized, P is also the average SNR. Eigen-beamforming is applied for the SU mode ($M = 1$), which transmits along the channel direction and is optimal for SU-MIMO with perfect CSIT [19]. ZF precoding is used for the MU mode ($1 < M \leq N_t$), as it is possible to derive closed-form results due to its simple structure, and it is optimal among the set of all linear precoders at asymptotically high SNR [4].

To assist the analysis, we assume that the channel $\mathbf{h}_u[n]$ is well modeled as a spatially white Gaussian channel, with entries $h_i[n] \sim \mathcal{CN}(0, 1)$. The investigation of other channel models is left to future work. We assume perfect channel state information (CSI) at the receiver, while the transmitter obtains CSI through limited feedback from the receiver. In addition, there is delay in the available CSIT. The models of the CSI delay and limited feedback are presented as follows.

A. CSI Delay Model

We consider a stationary ergodic Gauss-Markov block fading regular process (or auto regressive model of order 1) [20, Sec. 16–1], where the channel remains constant for a symbol duration and changes from symbol to symbol according to

$$\mathbf{h}[n] = \rho \mathbf{h}[n-1] + \mathbf{e}[n], \quad (2)$$

where $\mathbf{e}[n]$ is the channel error vector, with independent and identically-distributed (i.i.d.) entries $e_i[n] \sim \mathcal{CN}(0, \epsilon_c^2)$, uncorrelated with $\mathbf{h}[n-1]$, and i.i.d. in time. We assume the CSI delay is one symbol period, but the results can be easily extended to the case with delays of multiple

symbols. For the numerical analysis, we use a Gauss-Markov “fit” of the classical Clarke’s isotropic scattering model [21], as the true Clarke’s model is complicated for analysis. Then the correlation coefficient is $\rho = J_0(2\pi f_d T_s)$ with Doppler spread f_d , where T_s is the symbol duration and $J_0(\cdot)$ is the zero-th order Bessel function of the first kind. The variance of the error vector is $\epsilon_e^2 = 1 - \rho^2$. The value $f_d T_s$ is the normalized Doppler frequency. As shown in [8], the behaviors are different for the Clarke’s and Gauss-Markov model, especially at high SNR. However, the impact of channel quantization still persists and dominates at high SNR, so the conclusion in the paper still holds. In addition, the analysis for the Gauss-Markov model can be extended for the estimation or prediction error, which makes our results more general.

B. Channel Quantization

The channel direction information is fed back using a quantization codebook known at both the transmitter and receiver. The quantization is chosen from a codebook of unit norm vectors of size $L = 2^B$. Each user is assumed to have a different codebook to avoid users sharing the same quantization vector³. The codebook for user u is $\mathcal{C}_u = \{\mathbf{c}_{u,1}, \mathbf{c}_{u,2}, \dots, \mathbf{c}_{u,L}\}$. Each user quantizes its channel direction to the closest codeword, measured by the inner product. Therefore, the index of channel for user u is

$$I_u = \arg \max_{1 \leq \ell \leq L} |\tilde{\mathbf{h}}_u^* \mathbf{c}_{u,\ell}|, \quad (3)$$

where $\tilde{\mathbf{h}}_u = \frac{\mathbf{h}_u}{\|\mathbf{h}_u\|}$ is the channel direction. Random vector quantization (RVQ) [6], [22] is used to facilitate the analysis, where each quantization vector is independently chosen from the isotropic distribution on the N_t -dimensional unit sphere. We analyze performance averaged over realizations of all such random codebooks in addition to averaging over the fading distribution. It was shown in [23] that the RVQ-based codebook is asymptotically optimal in probability as $N_t, B \rightarrow \infty$, with $\frac{B}{N_t}$ keeping a constant.

Let $\cos \theta_u = |\tilde{\mathbf{h}}_u^* \hat{\mathbf{h}}_u|$, where $\theta_u = \angle(\tilde{\mathbf{h}}_u, \hat{\mathbf{h}}_u)$, then we have [24]

$$\xi_u = \mathbb{E}_{\theta_u} [\cos^2 \theta_u] = 1 - L_{i,j} \cdot \beta \left(2^B, \frac{N_t}{N_t - 1} \right), \quad (4)$$

where $\beta(x, y)$ is the Beta function, i.e. $\beta(x, y) = \frac{\Gamma(x)\Gamma(y)}{\Gamma(x+y)}$ with $\Gamma(x) = \int_0^\infty t^{x-1} e^{-t} dt$ as the Gamma function.

³A low-complexity method to generate different codebooks for different users is to first generate a common codebook, and then the codebook for each user is generated through random unitary rotation of this common codebook

III. THROUGHPUT ANALYSIS AND MODE SELECTION

In this section, we derive average achievable rates for different transmission modes. It is shown that the number of active users to maximize the sum throughput is closely related to transmit array gain, spatial division multiplexing gain, and residual inter-user interference. MMT is proposed to adaptively select the active mode to balance between these effects and maximize the throughput. For a selected mode M^* , M^* users will be selected based on channel-independent scheduling algorithms such as round-robin scheduling. The scheduling algorithm will be further discussed in Section IV.

A. Perfect CSIT

We first consider the system with perfect CSIT, which serves as the basis for the analysis of the impact of imperfect CSIT.

1) *SU-MIMO (Eigen-beamforming)*, $M = 1$: With perfect CSIT, the beamforming (BF) vector is the channel direction, i.e. $\mathbf{f}[n] = \tilde{\mathbf{h}}[n]$. The average throughput is the same as that of a maximal ratio combining diversity system, given in [25] as

$$\begin{aligned} R_{CSIT}(1) &= R_{BF}(\gamma, N_t) \triangleq \mathbb{E}_{\mathbf{h}} [\log_2 (1 + \gamma |\mathbf{h}^*[n] \mathbf{f}[n]|^2)] \\ &= \log_2(e) e^{1/\gamma} \sum_{k=0}^{N_t-1} \frac{\Gamma(-k, 1/\gamma)}{\gamma^k}, \end{aligned} \quad (5)$$

where $\Gamma(\alpha, x) = \int_x^\infty t^{\alpha-1} e^{-t} dt$ is the complementary incomplete gamma function, and $R_{BF}(\gamma, n)$ is the rate function for the diversity system with SNR γ and diversity order n . The BF system provides transmit array gain N_t as $\mathbb{E}_{\mathbf{h}} [\gamma |\mathbf{h}^*[n] \mathbf{f}[n]|^2] = N_t \gamma$. The array gain is defined as the increase in the average combined SNR over the average SNR on each branch [26].

2) *MU-MIMO (Zero-forcing)*, $1 < M \leq N_t$: The received SINR for the u -th user in a linear precoding MU-MIMO system in mode M is given by

$$\text{SINR}_u(M) = \frac{\frac{\gamma}{M} |\mathbf{h}_u^*[n] \mathbf{f}_u[n]|^2}{1 + \frac{\gamma}{M} \sum_{v \neq u} |\mathbf{h}_u^*[n] \mathbf{f}_v[n]|^2}. \quad (6)$$

Denote $\mathbf{H}[n] = [\mathbf{h}_1[n], \mathbf{h}_2[n], \dots, \mathbf{h}_U[n]]^*$, and the pseudo-inverse of $\mathbf{H}[n]$ as $\mathbf{F}[n] = \mathbf{H}^\dagger[n] = \mathbf{H}^*[n] (\mathbf{H}[n] \mathbf{H}^*[n])^{-1}$. The ZF precoding vector for the u -th user is obtained by normalizing the u -th column of $\mathbf{F}[n]$. Therefore, $\mathbf{h}_u^*[n] \mathbf{f}_v[n] = 0$, $\forall u \neq v$, i.e. there is no inter-user interference and each user gets an equivalent interference-free channel. The SINR for the u -th user becomes

$$\text{SINR}_{ZF,u}(M) = \frac{\gamma}{M} |\mathbf{h}_u^*[n] \mathbf{f}_u[n]|^2. \quad (7)$$

Due to the isotropic nature of i.i.d. Rayleigh fading, such orthogonality constraints to precancel inter-user interference consume $M - 1$ degrees of freedom at the transmitter. As a result, the

effective channel gain of each parallel channel is a chi-square random variable with $2(N_t - M + 1)$ degrees of freedom [4], [27], i.e. $|\mathbf{h}_u^*[n]\mathbf{f}_u[n]|^2 \sim \chi_{2(N_t - M + 1)}^2$. Therefore, the channel for each user is equivalent to a diversity channel with order $(N_t - M + 1)$ and effective SNR $\frac{\gamma}{M}$. The average achievable rate for the u -th user in mode M is

$$R_{CSIT,u}(M) = R_{BF}\left(\frac{\gamma}{M}, N_t - M + 1\right), \quad (8)$$

The average achievable sum rate for the ZF system of mode M is

$$\begin{aligned} R_{CSIT}(M) &= \sum_{u=1}^M R_{CSIT,u}(M) \\ &\stackrel{(a)}{=} MR_{BF}\left(\frac{\gamma}{M}, N_t - M + 1\right). \end{aligned} \quad (9)$$

The equality (a) follows the homogeneous nature of the network. When $M = 1$, this reduces to (5).

3) *Mode Selection*: From (9), the system in mode M provides a spatial division multiplexing gain of M and an array gain of $(N_t - M + 1)$ for each user. As M increases, the achievable spatial division multiplexing gain increases but the array gain decreases. Therefore, there is a tradeoff between the achievable array gain and the spatial division multiplexing gain. From (9), the mode that achieves the highest throughput for the given average SNR can be determined as

$$M^* = \arg \max_{1 \leq M \leq N_t} R_{CSIT}(M). \quad (10)$$

Note that this is a very simple optimization problem, as only N_t values need to be computed and compared. This transmission strategy that adaptively adjusts the number of active users is denoted as *multi-mode transmission* (MMT).

B. Imperfect CSIT

In this section, we consider imperfect CSIT, including both delay and channel quantization. As it is difficult to derive the exact achievable rate for such a system, we provide accurate closed-form approximations for mode selection. The average achievable rate for the SU mode $M = 1$ in such a system is provided in [18].

For the MU mode with delay and quantization, the precoding vectors are designed based on the quantized channel directions with delay, which achieve $\hat{\mathbf{h}}_u^*[n-1]\mathbf{f}_v^{(QD)}[n] = 0, \forall u \neq v$. Letters ‘ Q ’ and ‘ D ’ denote parameters of the system with channel quantization (limited feedback) and delay, respectively. The SINR for the u -th user in mode M is given as

$$\gamma_{ZF,u}^{(QD)}(M) = \frac{\frac{P}{M}|\mathbf{h}_u^*[n]\mathbf{f}_u^{(QD)}[n]|^2}{1 + \frac{P}{M}\sum_{v \neq u} |\mathbf{h}_u^*[n]\mathbf{f}_v^{(QD)}[n]|^2}. \quad (11)$$

We assume the mobile users can perfectly estimate the noise and interference and feed back these information to the transmitter, so the achievable rate for the u -th user is given as

$$R_{QD,u}(M) = \mathbb{E}_\gamma \left[\log_2(1 + \gamma_{ZF,u}^{(QD)}(M)) \right]. \quad (12)$$

The same metric is used in [6], [9], [18].

We first analyze the signal term and the interference term in (11).

1) *Signal term:* First, we approximate the signal term as

$$\begin{aligned} P_S &= \frac{P}{M} |\mathbf{h}_u^*[n] \mathbf{f}_u^{(QD)}[n]|^2 = \frac{P}{M} |(\rho_u \mathbf{h}_u[n-1] + \mathbf{e}_u[n])^* \mathbf{f}_u^{(QD)}[n]|^2 \\ &\stackrel{(a)}{\approx} \frac{P}{M} |\rho_u \mathbf{h}_u^*[n-1] \mathbf{f}_u^{(QD)}[n]|^2 \\ &= \frac{P}{M} \left| \rho_u \|\mathbf{h}_u[n-1]\| \cdot \tilde{\mathbf{h}}_u^*[n-1] \mathbf{f}_u^{(QD)}[n] \right|^2 \\ &\stackrel{(b)}{=} \frac{P}{M} \rho_u^2 \|\mathbf{h}_u[n-1]\|^2 \cdot \left| (\cos \theta_u \hat{\mathbf{h}}_u[n-1] + \sin \theta_u \mathbf{g}_u[n-1])^* \mathbf{f}_u^{(QD)}[n] \right|^2 \\ &\stackrel{(c)}{\approx} \frac{P}{M} \xi_u \rho_u^2 \|\mathbf{h}_u[n-1]\|^2 \cdot \left| \hat{\mathbf{h}}_u^*[n-1] \mathbf{f}_u^{(QD)}[n] \right|^2, \end{aligned} \quad (13)$$

where step (a) removes $\mathbf{e}_u^*[n] \mathbf{f}_u^{(QD)}[n]$, which is normally very small compared with the remaining term. In step (b), we write $\tilde{\mathbf{h}}_u[n-1] = (\cos \theta_u) \hat{\mathbf{h}}_u[n-1] + (\sin \theta_u) \mathbf{g}_u[n-1]$, where $\theta_u = \angle(\tilde{\mathbf{h}}_u[n-1], \hat{\mathbf{h}}_u[n-1])$ and $\mathbf{g}_u[n-1]$ is orthogonal to $\hat{\mathbf{h}}_u[n-1]$. Step (c) approximates the actual channel direction by the quantized version, which is justified for small quantization error, and approximates $\cos \theta_u^2$ by its expectation ξ_u , with ξ_u given in (4). As the quantized channel direction $\hat{\mathbf{h}}_u[n-1]$ is independent of each other, and $\mathbf{f}_u^{(QD)}[n]$ is designed to lie in the nullspace of $\hat{\mathbf{h}}_v[n-1]$, $\forall v \neq u$, similar to the case of perfect CSIT, $\|\mathbf{h}_u[n-1]\| \cdot \left| \hat{\mathbf{h}}_u^*[n-1] \mathbf{f}_u^{(QD)}[n] \right|^2 \sim \chi_{2(N_t - M + 1)}^2$. So as the perfect CSIT case it also provides an array gain of $N_t - M + 1$ for each user.

2) *Interference Term:* The residual interference term can be approximated as

$$\begin{aligned} &\frac{P}{M} \sum_{v \neq u} |\mathbf{h}_u^*[n] \mathbf{f}_v^{(QD)}[n]|^2 \\ &= \frac{P}{M} \sum_{v \neq u} |(\rho_u \mathbf{h}_u[n-1] + \mathbf{e}_u[n])^* \mathbf{f}_v^{(QD)}[n]|^2 \\ &\approx \frac{P}{M} \sum_{v \neq u} \rho_u^2 |\mathbf{h}_u^*[n-1] \mathbf{f}_v^{(QD)}[n]|^2 + \frac{P}{M} \sum_{v \neq u} |\mathbf{e}_u^*[n] \mathbf{f}_v^{(QD)}[n]|^2. \end{aligned} \quad (14)$$

The approximation for the denominator comes from removing the terms with both $\mathbf{e}_u[n]$ and $\mathbf{f}_v^{(QD)}[n]$. As shown in [18], the interference term due to quantization, $|\mathbf{h}_u^*[n-1] \mathbf{f}_v^{(QD)}[n]|^2$, can be well approximated as an exponential random variable with mean $\delta = 2^{-\frac{B}{N_t - 1}}$. The interference term due to delay, $|\mathbf{e}_u^*[n] \mathbf{f}_v^{(QD)}[n]|^2$, is also an exponential random variable with mean $\epsilon_{e,u}^2$ as $\mathbf{e}_u[n] \sim \mathcal{CN}(\mathbf{0}, \epsilon_{e,u}^2 \mathbf{I})$, $|\mathbf{f}_v[n]|^2 = 1$.

Based on the analysis and following the results in [6], [8], we can derive an upper bound for the rate loss for the u -th user due to imperfect CSIT, stated in the following theorem.

Theorem 1 (Rate loss): The rate loss for the u -th user with imperfect CSIT compared to that with perfect CSIT is upper bounded by

$$R_{CSIT,u} - R_{QD,u} \leq \log_2 \Delta_u^{(QD)}, \quad (15)$$

where $\Delta_u^{(QD)}$ is the average noise plus residual interference, given by

$$\begin{aligned} \Delta_u^{(QD)} &= \mathbb{E} \left[1 + \frac{P}{M} \sum_{v \neq u} |\mathbf{h}_u^*[n] \mathbf{f}_v^{(QD)}[n]|^2 \right] \\ &= 1 + \left(1 - \frac{1}{M} \right) P \left(\rho_u^2 2^{-\frac{B}{N_t-1}} + \epsilon_{e,u}^2 \right). \end{aligned} \quad (16)$$

Proof: The average noise plus interference $\Delta_u^{(QD)}$ can be derived based on the distribution of the interference term and following the approach in [18], which gives

$$\begin{aligned} &\mathbb{E} |\mathbf{h}_u^*[n] \mathbf{f}_v^{(QD)}[n]|^2 \\ &= \mathbb{E} |\rho_u \mathbf{h}_u^*[n-1] \mathbf{f}_v^{(QD)}[n]|^2 + \mathbb{E} |\mathbf{e}_u^*[n] \mathbf{f}_v^{(QD)}[n]|^2 \\ &= \rho_u^2 \cdot 2^{-\frac{B}{N_t-1}} + \epsilon_{e,u}^2. \end{aligned}$$

The upper bound is obtained by following the approach in [6], [8]. ■

Remark 1: From (16), we see that residual interference/rate loss depends on delay, codebook size, N_t , and M . It increases with delay, and decreases with codebook size. It also increases with P , which makes the system interference-limited at high SNR. With other parameters fixed, the residual interference increases as M increases, which means it may not be desirable to serve too many users.

The bound analysis in (15) provides helpful insights on the effects of different system parameters on the rate loss, but it is not accurate enough for mode selection. To accurately characterize the achievable rate, we derive the closed-form approximation for the MU mode in the following theorem.

Theorem 2 (Average achievable throughput): The average achievable rate for the u -th user in the MU system of mode M ($M > 1$) with both delay and channel quantization can be approximated by

$$R_{QD,u}(M) \approx \log_2(e) \sum_{i=0}^{N_t-L-1} \sum_{j=1}^2 \sum_{k=0}^{L-1} \sum_{l=0}^i \frac{a_k^{(j)} (l+k)!}{l!(i-l)!} \alpha^{l+k-i+1} I_1 \left(\frac{1}{\alpha}, \frac{\alpha}{\delta_j}, i, l+k+1 \right), \quad (17)$$

where $\alpha = \frac{\xi_u \rho_u^2 P}{M}$, $\delta_1 = \frac{\rho_u^2 P \delta}{M}$, $\delta_2 = \frac{\epsilon_{e,u}^2 P}{M}$, $L = M - 1$, $a_i^{(1)}$ and $a_i^{(2)}$ are given in (26) and (27), and $I_1(\cdot, \cdot, \cdot, \cdot)$ is the integral given in (30) in Appendix A.

Proof: See Appendix A. ■

Remark 2: To calculate (17) for a given user, we need only information about its correlation coefficient ($\rho_u^2 = 1 - \epsilon_{e,u}^2$), codebook size (B), and average SNR (P). Such information is normally fixed or changes slowly. Each user can feed back and update its own information, and then the BS can calculate the achievable rate. Instead, each user may also calculate the achievable rate and feeds back the preferred mode index. Note that the calculation and the mode selection is only done when the parameter changes, such as path loss change due to mobility.

As special cases, the average achievable rate for the system with delay or limited feedback is provided as follows.

Corollary 1: The average achievable rate for the u -th user in the delayed/limited-feedback system of mode M ($M > 1$) can be approximated by

$$R_u(M) \approx \log_2(e) \sum_{i=0}^{N_t-L-1} \sum_{l=0}^i \binom{L+l-1}{l} \frac{\alpha^{L+l-i}}{\beta^{L(i-l)!}} \cdot I_1\left(\frac{1}{\alpha}, \frac{\alpha}{\beta}, i, L+l\right), \quad (18)$$

where $L = M - 1$, $\alpha = \frac{\kappa P}{M}$, $\beta = \frac{(1-\kappa)P}{M}$, with

$$\kappa = \begin{cases} \rho^2 & \text{with delay only} \\ 1 - \delta & \text{with limited feedback only.} \end{cases} \quad (19)$$

and $I_1(\cdot, \cdot, \cdot, \cdot)$ is given in (30) in Appendix A.

Proof: See Appendix B. ■

In the following, we provide high SNR approximations for MU modes that can be used to analyze the performance in the interference-limited region.

Theorem 3 (High SNR approximation): The average achievable rate for the u -th user in the system with both delay and channel quantization in the MU mode $M > 1$ at high SNR is approximated as

$$R_{QD,u}^h(M) \approx \log_2(e) \sum_{i=0}^{N_t-L-1} \sum_{j=1}^2 \sum_{k=0}^{L-1} \frac{a_k^{(j)} \hat{\alpha}^{k+1} (k+i)!}{i!} I_2\left(\frac{\hat{\alpha}}{\hat{\delta}_j}, i, k+i+1\right), \quad (20)$$

where $\hat{\alpha} = \rho_u^2$, $a_i^{(1)}$ and $a_i^{(2)}$ are given in (26) and (27) with $\hat{\delta}_1 = \rho_u^2 \delta$, $\hat{\delta}_2 = \epsilon_{e,u}^2$, $L = M - 1$, and $I_2(\cdot, \cdot, \cdot)$ is the integral

$$I_2(a, m, n) = \int_0^\infty \frac{x^m}{(x+a)^n(x+1)} dx, \quad (21)$$

for which a closed-form expression can be found in [28, Sec. 3.8].

Proof: See Appendix C. ■

The high SNR result for the system with delay or limited feedback is provided in the following corollary.

Corollary 2: The achievable sum rate for the u -th user in the delayed/limited feedback system in MU mode $M > 1$ at high SNR is approximated as

$$R_{D,u}^h(M) \approx \log_2(e) \sum_{i=0}^{N_t-L-1} \binom{L+i-1}{i} \hat{\alpha}^L I_2(\hat{\alpha}, i, L+i), \quad (22)$$

where $\hat{\alpha} = \frac{\rho_u^2}{\epsilon_{e,u}^2}$ for delayed system, and $\hat{\alpha} = \frac{1-\delta}{\delta}$ for limited feedback system, $L = M - 1$, and $I_2(\cdot, \cdot, \cdot)$ is given in (21).

Proof: Following the steps in Appendix C with $\delta_1 = 0$. ■

Based on (17) and the approximation for the beamforming system in [18], the active mode that achieves the highest average throughput in the system with both delay and channel quantization is selected according to

$$M^* = \arg \max_{1 \leq M \leq N_t} R_{QD}(M), \quad (23)$$

where $R_{QD}(M) = \sum_{u=1}^M R_{QD,u}(M)$, with $R_{QD,u}(M)$ given in (17).

Remark 3: Considering (16), (13), and (17), the mode M is now related to residual interference, transmit array gain, and spatial division multiplexing gain. The idea of MMT is to balance between these effects to maximize the system throughput. The mode selection is based on fixed system parameters – the number of transmit antennas and the codebook size – and slow time-varying channel information – average SNR and normalized Doppler frequency.

To show the accuracy of the derived approximations, numerical results are provided in Fig. 1 for different modes, with $N_t = 4$, $B = 18$ bits, $v = 10$ km/hr, and $T_s = 1$ msec. We see that the approximation is very accurate at low to medium SNRs. At high SNR, when the sum rate of the MU mode saturates, the approximation becomes a lower bound, and the accuracy decreases as M increases. Interestingly, we see that the mode $M = 3$ always provides a higher throughput than the full MU mode $M = 4$. This is due to the fact that the full mode has the highest level of residual interference, as shown in (16), while it provides no array gain. Therefore, it is desirable to serve fewer than N_t users. We see that MMT is able to provide a throughput gain around 2 bps/Hz over the dual-mode switching [18] at medium SNR.

It is easy to verify that the high SNR result (20) matches the approximation, and can predict the behavior in the interference-limited region. In Fig. 2, we plot $M^* = \arg \max_{M>1} R_{QD}^h(M)$ for different normalized Doppler frequency $f_d T_s$, i.e. the mode with the highest sum rate in the interference-limited region. We see that M^* is different for different $f_d T_s$. For $B = 10$ bits, the mode $M = 2$ always has the highest throughput in the considered $f_d T_s$ range, as it provides a higher array gain and has lower residual interference than the higher modes; for $B = 20$ bits, as the CSIT accuracy is improved compared to $B = 10$ bits, $M = 3$ has the highest rate at high SNR when $f_d T_s$ is small, but $M = 4$ still has a lower throughput; the highest mode $M = 4$

provides the highest throughput only for $B = 30$ bits and very small $f_d T_s$ ($< 10^{-2}$). So with both delay and channel quantization, the highest mode $M = N_t$ is normally not preferable.

IV. MULTI-MODE TRANSMISSION WITH ROUND-ROBIN SCHEDULING

For the MIMO-BC with linear precoding, the number of users that can be supported simultaneously is constrained by the number of transmit antennas, so we need to select and transmit to a subset of users in each time slot since typically $U \gg N_t$. Based on the throughput analysis in Section III, MMT can be easily combined with round-robin scheduling, where the scheduling is based on the selected transmission mode but not on the instantaneous CSI feedback. This scheduling algorithm is of low complexity, only requires instantaneous CSI feedback from a small number of users, and provides temporal fairness. It is suitable for delay sensitive services or can be applied when it is possible to get feedback only from few users.

We assume that the BS has knowledge of the average received SNR and the normalized Doppler frequency of each user, which can be fed back from users and do not require frequent update as they change slowly. Based on such information, the BS can estimate the average achievable throughput for each user for a given subset of selected users based on (17). All the users are indexed and ordered as user $1, 2, \dots, U$. Scheduling starts from the head of the user queue. Once a user is scheduled, it is moved to the tail of the user queue. In the given time slot, denote u_h as the index of the user at the head of the user queue, and \mathcal{S} as the subset of the selected users. The scheduling algorithm is given in Table I and also illustrated in Fig. 3. It is similar to the conventional round-robin scheduling and serves users in circular order, but in each time slot multiple users rather than a single user may be served. MMT is applied in each time slot, where the number of selected users is determined based on the analysis in Section III. Such user scheduling is denoted as *Multi-Mode Transmission (MMT) based scheduling*.

Remark 4: Note that for the homogeneous network where all the users have the same average SNR, normalized Doppler frequency, and number of feedback bits, the number of scheduled users in each time slot is fixed, denoted as M^* . The value of M^* is determined from (23), and then M^* users are selected from the head of the user queue. This is the main scenario considered in the paper, but the scheduling algorithm can be applied to heterogeneous networks as well.

Compared to opportunistic scheduling based on instantaneous CSI feedback, the proposed algorithm greatly reduces the amount of CSI feedback, as in each time slot only the selected M users ($M \ll U$) need to feed back their instantaneous CSI for the precoder design. In addition, as will be shown in numerical results, it provides performance close to the one with instantaneous CSI feedback from a large number of users. The proposed algorithm is suitable for other systems

with scheduling independent of the channel status, such as random selection or the ones based on the queue length.

V. NUMERICAL RESULTS

This section presents numerical results to demonstrate the performance of our proposed transmission strategy and to provide design guidelines in practical systems. We focus on a homogeneous network where all the users have i.i.d. channels. The number of transmit antennas at the BS is $N_t = 4$, which is the value currently implemented in broadband wireless standards such as 3GPP LTE.

A. Operating Region and Throughput Gain of Multi-mode Transmission

In this section, we consider parameters used in the 3GPP LTE (Long Term Evolution) standard [29], [30]. The Advanced Wireless Services (AWS) spectrum, which is one of the prime candidates for initial LTE deployment in the US, is considered, i.e. the carrier frequency is $f_c = 2.1$ GHz. In LTE, the minimum size of radio resource that can be allocated in the time domain is one subframe of 1 msec. Considering the propagation and processing time, the typical CSIT delay in the FDD mode is five subframes, i.e. the delay is $\tau = 5$ msec.

1) *Operating Regions*: Based on the results in Section III, the preferred mode M^* can be determined for a given scenario. Accordingly, the operating regions for different modes can be plotted for different system parameters. Fig. 4(a) and Fig. 4(b) show the operating regions for the system with both delay and channel quantization, for different mobility v and different feedback bits B , respectively, where each mark on the figure denotes the type of the active mode. There are several key observations:

- 1) For the given v and B , the SU mode ($M = 1$) will be active at both low and high SNRs, due to its array gain and the robustness to imperfect CSIT, respectively.
- 2) For MU modes to be active, v needs to be small while B needs to be large. Specifically, to activate $M = 2$, we need $v \leq 12$ km/hr with $B = 15$ bits as in Fig. 4(a), and need $B \geq 6$ bits with $v = 5$ km/hr as in Fig. 4(b); to activate $M = 3$, we need $v \leq 6$ km/hr with $B = 15$ bits and $B \geq 14$ bits with $v = 5$ km/hr. Note that in LTE each user only feeds back 4 bits to indicate its channel direction.
- 3) The full MU mode $M = N_t$ is not active at all with the considered parameters, as it suffers from the highest residual interference and does not provide array gain.

2) *SU-MIMO vs. MMT*: In Fig. 5, we compare MMT with ZF precoding (MMT-ZF) and the single-user beamforming (SU-BF) transmission, both with round-robin scheduling, and with

$f_c = 2.1$ GHz, $\tau = 5$ msec., and $v = 5$ km/hr. We see that for $B = 4$ the curves of MMT-ZF and SU-BF overlap, which means no MU mode is activated. This confirms the result in Fig. 4(b). For $B = 8$, MMT-ZF provides throughput gain over SU-BF for SNR in $0 \sim 18$ dB. For $B = 12$, MMT-ZF provides throughput gain for SNR in $-5 \sim 25$ dB, which is larger than 20% for SNR=10 \sim 20 dB.

3) *Delay vs. Quantization Error*: From the analysis of residual interference terms in Section III-B, we can determine for a given scenario which effect dominates, delay-mobility or channel quantization error. Each interference term due to delay-mobility has variance $\sigma_D^2 = \epsilon_{e,u}^2$, while each interference term due to channel quantization error has variance $\sigma_Q^2 = \rho_u^2 2^{-\frac{B}{N_t-1}}$. For example, for $v = 5$ km/hr, $f_c = 2.1$ GHz, and $\tau = 5$ msec, we have $\sigma_D^2 = 0.0458$, and $\sigma_Q^2 = 0.3787$ with $B = 4$, $\sigma_Q^2 = 0.1503$ with $B = 8$, so $\sigma_D^2 \ll \sigma_Q^2$ in these scenarios and the channel quantization error dominates the performance, as shown in Fig. 5; to get $\sigma_D^2 \approx \sigma_Q^2$, we need $B = 13$, but a too large B will not help much as delay-mobility will start to dominate. Fig. 6 shows the performance of ZF-MMT with different values of B . We see that the sum rate cannot be further improved once B is sufficiently large ($B > 20$).

Remark 5: The numerical results in this section provide the following insights:

- 1) As shown in Fig. 4(a), for a given delay and give B , the mobility plays a significant role, and MU-MIMO should only be used with low mobility (≤ 12 km/hr).
- 2) Both Fig. 4(b) and Fig. 5 show that the number of feedback bits in LTE ($B = 4$) is not large enough for MU-MIMO and should be increased ($B \geq 8$).
- 3) As CSI feedback occurs only in certain subframes, the delay in available CSIT is related to the radio frame length. Therefore, it is expected that the MU-MIMO is more applicable in the LTE system which has a shorter frame length (1 msec) than the WiMAX system (5 msec).
- 4) Reducing quantization error by increasing B is not enough to fully exploit the throughput gain of MU-MIMO, and other CSIT imperfections should be taken into consideration.

B. ZF vs. MMSE Precoding

MMSE precoding, or regularized ZF precoding, can increase the throughput at low SNR compared to ZF precoding [31]. Fig. 7 compares the sum rates of MMT-ZF and MMSE precoding. For the *perfect CSIT* case, the number of active users for MMSE precoding is fixed to be $U = N_t$, as little gain can be achieved by varying the user number. We see that the sum rates of the two systems are very close. This means that MMT improves the performance of ZF precoding and approaches that of MMSE precoding. With *imperfect CSIT*, simulation results for different modes

with MMSE precoding are plotted, showing that mode switching is also required to improve the spectral efficiency for MMSE precoding. If MMT is applied for both systems, we see that the performance of ZF precoding approaches that of MMSE precoding. Note that MMSE precoding requires instantaneous CSI feedback from all the user, while the number of users that need to feed back instantaneous CSI for ZF precoding depends on the active mode and normally is less than N_t . In addition, as MMSE precoding is difficult to analyze, the preferred mode cannot be easily determined. Therefore, employing MMT, ZF precoding is preferred to MMSE precoding.

C. MMT Under a Feedback Overload Constraint

In this section, we consider the scenario with a constraint on the total feedback overhead, i.e. the total number of feedback bits from all the users is fixed to be B_T [32]. We compare the proposed MMT-ZF with round-robin scheduling and the ZF precoding with opportunistic user selection (US-ZF) that is based on instantaneous CSI feedback. As shown in [32], with a feedback overhead constraint it is more desirable to get high-rate/high-quality feedback from a small number of users than low-rate/course feedback from a large number of users, and the optimal number of feedback bits from each user and the number of active users can be determined. We focus on the impact of limited feedback, and delay is not considered in this section. For MMT-ZF, the number of feedback bits for each user is $\lfloor \frac{B_T}{M} \rfloor$ for mode M . For US-ZF, the optimal feedback bits for each user, B_{US}^* , is obtained throughput simulation⁴, and $\lfloor \frac{B_T}{B_{US}^*} \rfloor$ users feed back their instantaneous CSI for scheduling.

Fig. 8 shows the performance of MMT-ZF and US-ZF, together with the PU²RC (Per Unitary basis stream User and Rate Control) [33] and single-user beamforming (SU-BF) with channel-dependent maximum rate scheduling. We see that MMT-ZF almost always performs better than both PU²RC and SU-BF, and its performance is close to US-ZF. At low SNR, PU²RC provides slightly higher throughput than MMT-ZF as it provides multiuser diversity, which is a kind of power gain and dominates the performance at low SNR. For a given SNR value, when B_T keeps increasing, the throughput of US-ZF increases due to multiuser diversity, while the sum rate of MMT-ZF saturates as the full mode $M = N_t$ is activated and there is limited performance gain to further improve the accuracy of CSIT.

⁴In [32], an approximation was derived to solve for B_{US}^* (eq. (11)). However, it is based on the rate loss derivation, and is not accurate especially for medium to high SNR values. The inaccuracy of the rate loss based result at high SNR was also shown in [18].

VI. CONCLUSIONS

In this paper, we propose a multi-mode transmission strategy that adaptively adjusts the number of active users based on the average achievable rate. Considering transmit array gain, spatial division multiplexing gain and residual inter-user interference, multi-mode transmission improves the spectral efficiency over SU-MIMO at medium SNR. It is shown that the full mode $M^* = N_t$ will normally not be activated as it has the highest residual interference and no array gain. Multi-mode transmission can be combined with round-robin scheduling to serve a large number of users, which selects users based on average SNR, codebook size, and normalized Doppler frequency. The proposed algorithm significantly reduces the feedback amount, and provides throughput close to the one based on instantaneous CSI feedback when there is a total feedback overhead constraint. The analysis and numerical results provide insights and design guidelines that are of practical importance.

APPENDIX

A. Proof of Theorem 2

Assuming interference terms are independent, and independent of the signal term, $\gamma_{ZF,u}^{(QD)}$ can be approximated as

$$\gamma_{ZF,u}^{(QD)} \approx \frac{\alpha z}{1 + \delta_1 y_1 + \delta_2 y_2} \triangleq x, \quad (24)$$

where $\alpha = \frac{\rho_u^2 P}{M}$, $\delta_1 = \frac{\rho_u^2 P \delta}{M}$, $\delta_2 = \frac{\epsilon_{e,u}^2 P}{M}$, $y_1 \sim \chi_{2L}^2$, $y_2 \sim \chi_{2L}^2$, $z \sim \chi_{2(N_t-L)}^2$, $L = M - 1$, and y_1 , y_2 , z are independent of each other.

Let $y = \delta_1 y_1 + \delta_2 y_2$, then the pdf of y , which is the sum of two independent chi-square random variables, is given as [34]

$$p_Y(y) = e^{-y/\delta_1} \sum_{i=0}^{L-1} a_i^{(1)} y^i + e^{-y/\delta_2} \sum_{i=0}^{L-1} a_i^{(2)} y^i = \sum_{j=1}^2 \sum_{k=0}^{L-1} a_k^{(j)} y^k e^{-y/\delta_j}, \quad (25)$$

where

$$a_i^{(1)} = \frac{1}{\delta_1^{i+1} (L-1)!} \left(\frac{\delta_1}{\delta_1 - \delta_2} \right)^L \frac{(2(L-1) - i)!}{i!(L-1-i)!} \left(\frac{\delta_2}{\delta_2 - \delta_1} \right)^{L-1-i}, \quad (26)$$

$$a_i^{(2)} = \frac{1}{\delta_2^{i+1} (L-1)!} \left(\frac{\delta_2}{\delta_2 - \delta_1} \right)^L \frac{(2(L-1) - i)!}{i!(L-1-i)!} \left(\frac{\delta_1}{\delta_1 - \delta_2} \right)^{L-1-i}. \quad (27)$$

We first derive the cumulative distribution function (cdf) of the random variable x as follows.

$$\begin{aligned}
F_X(x) &= P\left(\frac{\alpha z}{1+y} \leq x\right) = \int_0^\infty F_{Z|Y}\left(\frac{x}{\alpha}(1+y)\right) p_Y(y) dy \\
&= \int_0^\infty \left(1 - e^{-\frac{x}{\alpha}(1+y)} \sum_{i=0}^{N_t-L-1} \frac{\left[\frac{x}{\alpha}(1+y)\right]^i}{i!}\right) p_Y(y) dy \\
&= 1 - e^{-x/\alpha} \int_0^\infty \left\{ e^{-\frac{x}{\alpha}y} \sum_{i=0}^{N_t-L-1} \frac{\left[\frac{x}{\alpha}(1+y)\right]^i}{i!} \cdot \sum_{j=1}^2 \sum_{k=0}^{L-1} a_k^{(j)} y^k e^{-y/\delta_j} \right\} dy \\
&\stackrel{(a)}{=} 1 - e^{-x/\alpha} \sum_{i=0}^{N_t-L-1} \sum_{j=1}^2 \sum_{k=0}^{L-1} \frac{a_k^{(j)} (x/\alpha)^i}{i!} \sum_{l=0}^i \binom{i}{l} \int_0^\infty \exp\left[-\left(\frac{x}{\alpha} + \frac{1}{\delta_j}\right)y\right] y^{l+k} dy \\
&\stackrel{(b)}{=} 1 - \sum_{i=0}^{N_t-L-1} \sum_{j=1}^2 \sum_{k=0}^{L-1} \sum_{l=0}^i \frac{a_k^{(j)} (l+k)!}{l!(i-l)!} \cdot \frac{\alpha^{l+k-i+1} e^{-x/\alpha} x^i}{\left(x + \frac{\alpha}{\delta_j}\right)^{l+k+1}}, \tag{28}
\end{aligned}$$

where step (a) follows binomial expansion of $(y+1)^i$, and step (b) follows the equality $\int_0^\infty y^M e^{-\alpha y} = M! \alpha^{-(M+1)}$.

The expectation of $\ln(1+x)$ on x is derived as follows.

$$\begin{aligned}
\mathbb{E}_X[\ln(1+X)] &= \int_0^\infty \ln(1+x) dF_X \stackrel{(a)}{=} \int_0^\infty \frac{1-F_X(x)}{x+1} dx \\
&= \int_0^\infty \left[\sum_{i=0}^{N_t-L-1} \sum_{j=1}^2 \sum_{k=0}^{L-1} \sum_{l=0}^i \frac{a_k^{(j)} (l+k)!}{l!(i-l)!} \cdot \frac{\alpha^{l+k-i+1} e^{-x/\alpha} x^i}{\left(x + \frac{\alpha}{\delta_j}\right)^{l+k+1} (x+1)} dx \right] \\
&\stackrel{(b)}{=} \sum_{i=0}^{N_t-L-1} \sum_{j=1}^2 \sum_{k=0}^{L-1} \sum_{l=0}^i \frac{a_k^{(j)} (l+k)!}{l!(i-l)!} \alpha^{l+k-i+1} I_1\left(\frac{1}{\alpha}, \frac{\alpha}{\delta_j}, i, l+k+1\right), \tag{29}
\end{aligned}$$

where step (a) follows integration by parts and $I_1(\cdot, \cdot, \cdot, \cdot)$ in step (b) is given by

$$I_1(a, b, m, n) = \int_0^\infty \frac{x^m e^{-ax}}{(x+b)^n (x+1)} dx, \tag{30}$$

for which a closed-form expression can be found in [28, Sec. 3.8]. Then the achievable sum rate for the u -th user in mode M can be approximated as

$$R_{QD,u}(M) = \mathbb{E}_\gamma \left[\log_2(1 + \gamma_{ZF,u}^{(QD)}) \right] \approx \log_2(e) \cdot \mathbb{E}_X[\ln(1+X)],$$

which gives (17).

B. Proof of Corollary 1

For the system with delay, similar to (13), the received signal power for the u -th user is approximated as

$$P_S^{(D)} \approx \frac{P}{M} |\rho_u \mathbf{h}_u^*[n-1] \mathbf{f}_u[n]|^2. \tag{31}$$

Similar to (24), the received SINR can be approximated by

$$\gamma_{ZF,u}^{(D)} \approx \frac{\alpha z}{1 + \beta y} \triangleq x, \quad (32)$$

where $\alpha = \frac{\rho_u^2 P}{M}$, $\beta = \frac{\epsilon_{e,u}^2 P}{M}$, $y \sim \chi_{2L}^2$, $z \sim \chi_{2(N_t-L)}^2$, $L = M - 1$, and y, z are independent of each other.

For the system with limited feedback, similar to (13), we get the received signal power as

$$\begin{aligned} P_S^{(Q)} &= \frac{P}{M} |\mathbf{h}_u^*[n] \mathbf{f}_u^{(Q)}[n]|^2 \\ &= \frac{P}{M} \|\mathbf{h}_u[n]\|^2 \cdot |(\cos \theta_u) \hat{\mathbf{h}}_u^*[n] \mathbf{f}_u^{(Q)}[n] + (\sin \theta_u) \mathbf{g}_u^*[n] \mathbf{f}_u^{(Q)}[n]|^2 \\ &\stackrel{(a)}{\approx} \frac{P}{M} \|\mathbf{h}_u[n]\|^2 \cdot |(\cos \theta_u) \hat{\mathbf{h}}_u^*[n] \mathbf{f}_u^{(Q)}[n]|^2 \\ &\stackrel{(b)}{\approx} \frac{P}{M} \|\mathbf{h}_u[n]\|^2 \cdot \mathbb{E}_\theta[\cos^2 \theta_u] \cdot |\hat{\mathbf{h}}_u^*[n] \mathbf{f}_u^{(Q)}[n]|^2, \end{aligned} \quad (33)$$

where in step (a) we remove the term with $\sin \theta_u$ which is small for a large B , and in step (b) we approximate $\cos^2 \theta_u$ by $\mathbb{E}_\theta[\cos^2 \theta_u]$. As shown in [6], $\mathbb{E}_\theta[\cos^2 \theta_u]$ is well approximated by $1 - \delta$, with $\delta = 2^{-\frac{B}{N_t-1}}$. Then the received SINR for the u -th user is approximated by

$$\gamma_{ZF,u}^{(Q)} \approx \frac{\alpha z}{1 + \beta y} \triangleq x, \quad (34)$$

where $\alpha = \frac{(1-\delta)P}{M}$, $\beta = \frac{\delta P}{M}$, $y \sim \chi_{2L}^2$, $z \sim \chi_{2(N_t-L)}^2$, $L = M - 1$, and y, z are independent of each other.

From (32) and (34), we can get the result in (18) following the steps in Appendix A.

C. Proof of Theorem 3

From (24), the received SINR for the u -th user at high SNR is approximated by

$$\gamma_{ZF,u}^{(D)} \approx \frac{\hat{\alpha} z}{\hat{\delta}_1 y_1 + \hat{\delta}_2 y_2},$$

where $\hat{\alpha} = \rho_u^2$, $\hat{\delta}_1 = \rho_u^2 \delta$, $\hat{\delta}_2 = \epsilon_{e,u}^2$, $z \sim \chi_{2(N_t-L)}^2$, $y_1 \sim \chi_{2L}^2$, $y_2 \sim \chi_{2L}^2$, $L = M - 1$, and z, y_1 and y_2 are independent.

Denote $x = \frac{\hat{\alpha} z}{\hat{\delta}_1 y_1 + \hat{\delta}_2 y_2}$, following the same steps as in Appendix A, the cdf of x is derived as

$$F_X(x) = 1 - \sum_{i=0}^{N_t-L-1} \sum_{j=1}^2 \sum_{k=0}^{L-1} \frac{a_k^{(j)} \hat{\alpha}^{k+1} (k+i)!}{i!} \cdot \frac{x^i}{\left(x + \frac{\hat{\alpha}}{\hat{\delta}_j}\right)^{k+i+1}}. \quad (35)$$

Then following the steps in (29) we get the result in (20).

REFERENCES

- [1] D. Gesbert, M. Kountouris, R. W. Heath Jr., C. B. Chae, and T. Sälzer, "Shifting the MIMO paradigm: From single user to multiuser communications," *IEEE Signal Processing Magazine*, vol. 24, no. 5, pp. 36–46, Sept. 2007.
- [2] A. Lapidoth, S. Shamai, and M. Wigger, "On the capacity of fading MIMO broadcast channels with imperfect transmitter side-information," in *Proc. Allerton Conference on Communication, Control and Computing*, Monticello, IL, Sept. 2005.
- [3] T. Yoo and A. Goldsmith, "On the optimality of multi-antenna broadcast scheduling using zero-forcing beamforming," *IEEE J. Select. Areas Commun.*, vol. 24, no. 3, pp. 528–541, Mar. 2006.
- [4] J. Lee and N. Jindal, "High SNR analysis for MIMO broadcast channels: Dirty paper coding vs. linear precoding," *IEEE Trans. Inform. Theory*, vol. 53, no. 12, pp. 4787–4792, Dec. 2007.
- [5] D. J. Love, R. W. Heath Jr., V. K. N. Lau, D. Gesbert, B. D. Rao, and M. Andrews, "An overview of limited feedback in wireless communication systems," *IEEE J. Select. Areas Commun.*, vol. 26, no. 8, pp. 1341–1365, Oct. 2008.
- [6] N. Jindal, "MIMO broadcast channels with finite rate feedback," *IEEE Trans. Inform. Theory*, vol. 52, no. 11, pp. 5045–5059, Nov. 2006.
- [7] T. Yoo, N. Jindal, and A. Goldsmith, "Multi-antenna downlink channels with limited feedback and user selection," *IEEE J. Select. Areas Commun.*, vol. 25, no. 7, pp. 1478–1491, Sept. 2007.
- [8] G. Caire, N. Jindal, M. Kobayashi, and N. Ravindran, "Multiuser MIMO achievable rates with downlink training and channel state feedback," *IEEE Trans. Inform. Theory*, to appear, available on <http://arxiv.org/abs/0711.2642>.
- [9] P. Ding, D. J. Love, and M. D. Zoltowski, "Multiple antenna broadcast channels with partial and limited feedback," *IEEE Trans. Signal Processing*, vol. 55, no. 7, pp. 3417–3428, Jul. 2007.
- [10] K. Huang, R. W. Heath Jr., and J. G. Andrews, "Space division multiple access with a sum feedback rate constraint," *IEEE Trans. Signal Processing*, vol. 55, no. 7, pp. 3879–3891, Jul. 2007.
- [11] R. W. Heath Jr., T. Wu, and A. C. K. Soong, "Progressive refinement for high resolution limited feedback beamforming," *EURASIP Journal on Advances in Signal Processing*, 2009, article ID 463823, 13 pages.
- [12] R. W. Heath Jr. and A. J. Paulraj, "Switching between diversity and multiplexing in MIMO systems," *IEEE Trans. Commun.*, vol. 53, no. 6, pp. 962–968, Jun. 2005.
- [13] D. J. Love and R. W. Heath Jr., "Limited feedback unitary precoding for orthogonal space-time block codes," *IEEE Trans. Signal Processing*, vol. 53, no. 1, pp. 64–73, Jan. 2005.
- [14] C. K. Au-Yeung, S. Y. Park, and D. J. Love, "A simple dual-mode limited feedback multiuser downlink system," *IEEE Trans. Commun.*, vol. 57, no. 5, pp. 1514–1522, May 2009.
- [15] M. Kountouris, D. Gesbert, and T. Sälzer, "Distributed transmit mode selection for MISO broadcast channels with limited feedback: Switching from SDMA to TDMA," in *Proc. IEEE Workshop on Signal Processing Advances in Wireless Communications (SPAWC 2008)*, Recife, Brazil, Jul. 2008, pp. 371–375.
- [16] C. Lee, C. B. Chae, S. Vishwanath, and R. W. Heath Jr., "Adaptive mode switching in correlated multiple antenna cellular networks," *Journal of Communications and Networks*, vol. 11, no. 3, pp. 279–286, Jun. 2009.
- [17] W. Dai, Y. Liu, B. C. Rider, and W. Gao, "How many users should be turned on in a multi-antenna broadcast channel?" *IEEE J. Select. Areas Commun.*, vol. 26, no. 8, pp. 1526–1535, Oct. 2008.
- [18] J. Zhang, R. W. Heath Jr., M. Kountouris, and J. G. Andrews, "Mode switching for the multi-antenna broadcast channel based on delay and channel quantization," *EURASIP Journal on Advances in Signal Processing*, 2009, article ID 802548, 14 pages.
- [19] I. E. Telatar, "Capacity of multi-antenna Gaussian channels," *Europ. Trans. Telecommun.*, vol. 10, pp. 585–595, Nov. 1999.
- [20] S. Haykin, *Adaptive Filter Theory*, 3rd ed. Englewood Cliffs, NJ: Prentice-Hall, 1996.
- [21] R. H. Clarke, "A statistical theory of mobile radio reception," *Bell System Tech. J.*, vol. 47, pp. 957–1000, 1968.
- [22] W. Santipach and M. Honig, "Asymptotic capacity of beamforming with limited feedback," in *Proc. IEEE Int. Symp. Information Theory*, Chicago, IL, Jun./Jul. 2004, p. 290.

TABLE I
SCHEDULING ALGORITHM

- 1) Initially, set $\mathcal{S} = \{u_h\}$, $R_{old} = R_{QD}(u_h)$, $\hat{u} = u_h$.
- 2) While $|\hat{u} - u_h| < N_t$
 - a) $\hat{\mathcal{S}} = \hat{\mathcal{S}} + \{\hat{u} + 1 \bmod U\}$.
 - b) Calculate $R_{new} = \sum_{s \in \hat{\mathcal{S}}} R_{QD,s}(\hat{\mathcal{S}})$.
 - c) If $R_{new} > R_{old}$, set $R_{old} = R_{new}$, $\mathcal{S} = \hat{\mathcal{S}}$
 - d) Set $\hat{u} = \hat{u} + 1 \bmod U$.
- 3) Let $u_h = u_h + |\mathcal{S}| \bmod U$.

- [23] W. Dai, Y. Liu, and B. Rider, "Quantization bounds on Grassmann manifolds and applications in MIMO systems," *IEEE Trans. Inform. Theory*, vol. 54, no. 3, pp. 1108–1123, Mar. 2008.
- [24] C. K. Au-Yeung and D. J. Love, "On the performance of random vector quantization limited feedback beamforming in a MISO system," *IEEE Trans. Wireless Commun.*, vol. 6, no. 2, pp. 458–462, Feb. 2007.
- [25] M. Alouini and A. Goldsmith, "Capacity of Rayleigh fading channels under different adaptive transmission and diversity-combining techniques," *IEEE Trans. Veh. Technol.*, vol. 48, no. 4, pp. 1165–1181, Jul. 1999.
- [26] A. Goldsmith, *Wireless Communications*. Cambridge University Press, 2005.
- [27] N. Jindal, J. Andrews, and S. Weber, "Multi-antenna communication in ad hoc networks: Achieving MIMO gains with SIMO transmission," *IEEE Trans. Commun.*, Dec. 2009, submitted, available on <http://arxiv.org/abs/0809.5008>.
- [28] J. Zhang, "Adapting MIMO networks to manage interference," Ph.D. dissertation, University of Texas at Austin, Austin, TX, Dec. 2009.
- [29] 3GPP TR 36.913 V8.0.1, "Requirements for further advancements for Evolved Universal Terrestrial Radio Access (E-UTRA) (LTE-Advanced) (Release 8)," Mar. 2009.
- [30] 3GPP TS 36.211 V8.5.0, "Evolved Universal Terrestrial Radio Access (E-UTRA); Physical Channels and Modulation (Release 8)," Dec. 2008.
- [31] C. Peel, B. Hochwald, and A. Swindlehurst, "Vector-perturbation technique for near-capacity multiantenna multiuser communication-Part I: Channel inversion and regularization," *IEEE Trans. Commun.*, vol. 53, no. 1, pp. 195–202, Jan. 2005.
- [32] N. Ravindran and N. Jindal, "Multi-user diversity vs. accurate channel state information in MIMO downlink channels," *submitted to IEEE Trans. Communications*, Jul. 2009.
- [33] K. Huang, J. G. Andrews, and R. W. Heath Jr., "Performance of orthogonal beamforming for SDMA with limited feedback," *IEEE Trans. Veh. Technol.*, vol. 58, no. 1, pp. 152–164, Jan. 2009.
- [34] M. K. Simon, *Probability Distributions Involving Gaussian Random Variables: A Handbook for Engineers and Scientists*. Springer, 2002.

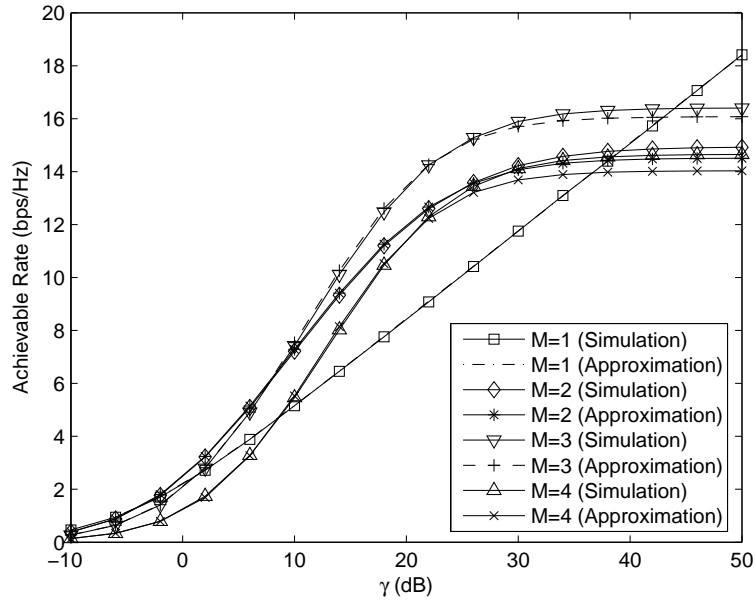


Fig. 1. Simulation results and approximations for different M , $N_t = 4$, $v = 10$ km/hr, $T_s = 1$ msec, $B = 18$ bits.

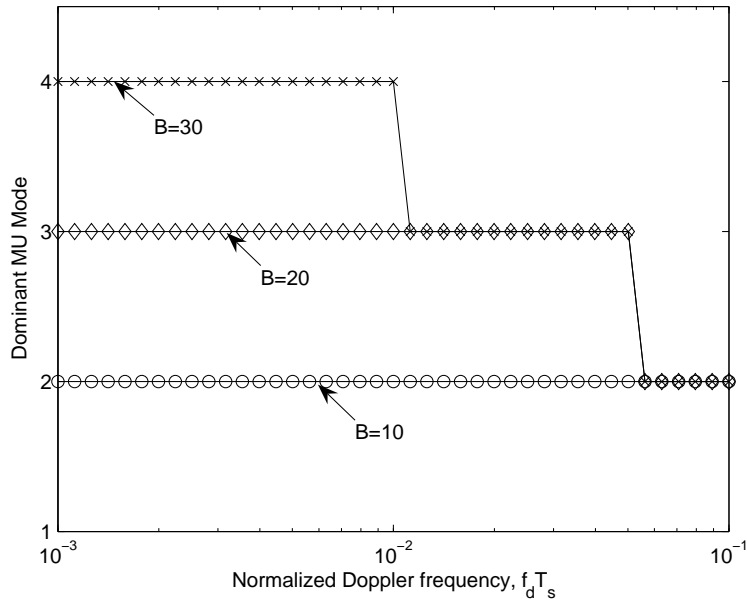


Fig. 2. The MU mode with the highest rate ceiling for different $f_d T_s$, with $N_t = 4$.

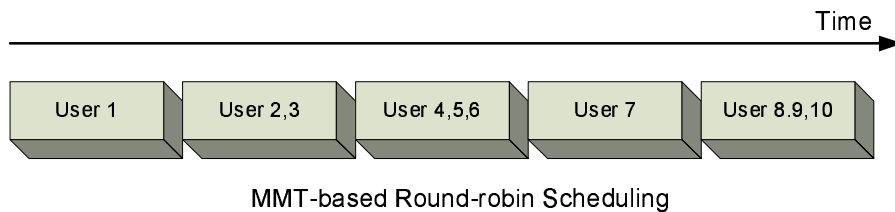
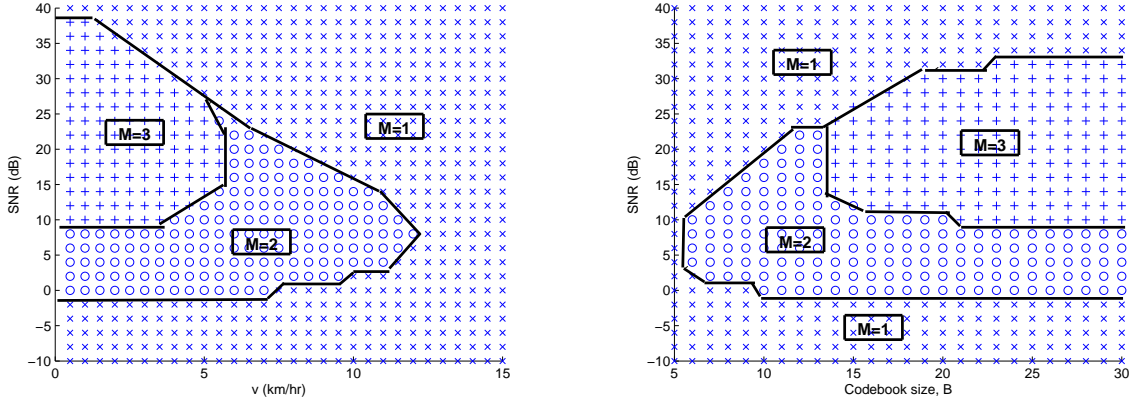


Fig. 3. Illustration of multi-mode transmission (MMT) based round-robin scheduling.



(a) Different v , $f_c = 2.1$ GHz, $\tau = 5$ msec, $B = 15$ bits. (b) Different B , $f_c = 2.1$ GHz, $\tau = 5$ msec., and $v = 5$ km/hr.

Fig. 4. Operating regions for different modes with both CSI delay and channel quantization, $N_t = 4$. The mode $M = i$ means that there are i active users. In this plot, 'x' is for $M = 1$, 'o' is for $M = 2$, '+' is for $M = 3$, and '□' is for $M = 4$. Note that the highest mode $M = 4$ is never activated in both figures.

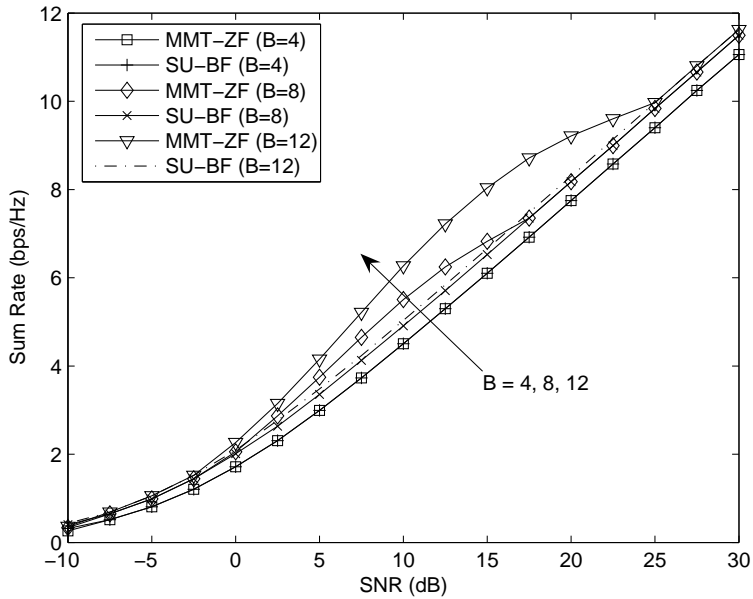


Fig. 5. Simulation results of SU-BF and MMT-ZF with different B , $N_t = 4$, $f_c = 2.1$ GHz, $\tau = 5$ msec., and $v = 5$ km/hr.

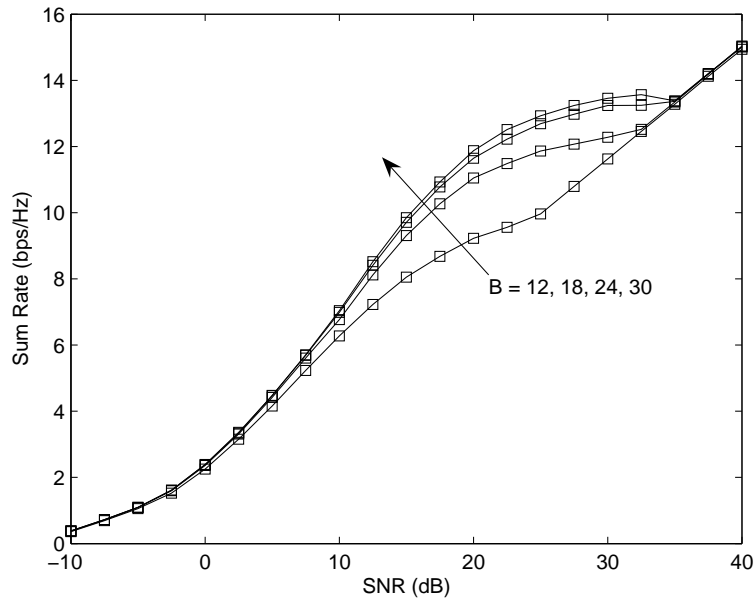


Fig. 6. Performance of MMT-ZF with different B , $N_t = 4$, $f_c = 2.1$ GHz, $\tau = 5$ msec., and $v = 5$ km/hr.

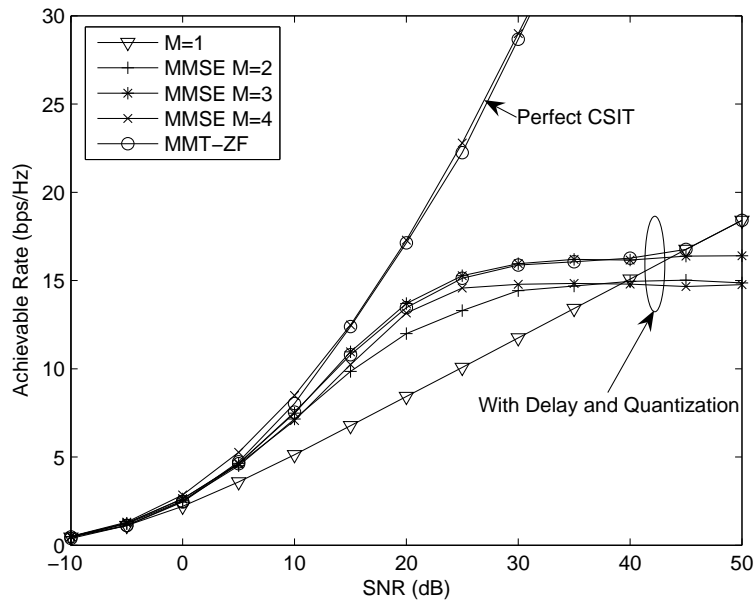


Fig. 7. Simulation results of MMSE precoding and MMT-ZF systems, $N_t = 4$. For imperfect CSIT, $B = 18$ bits, $f_c = 2.1$ GHz, $\tau = 5$ msec., and $v = 5$ km/hr.

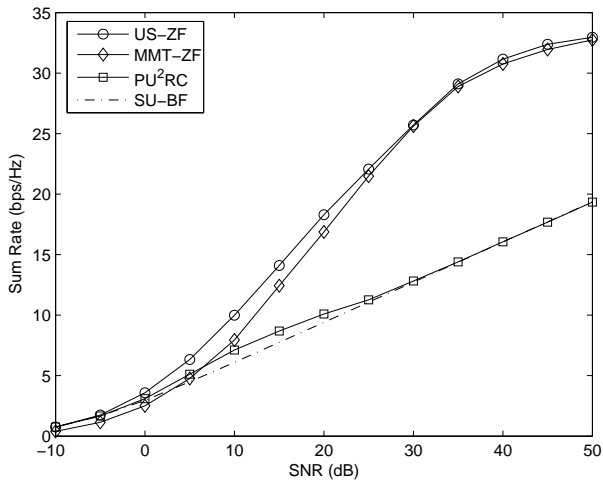
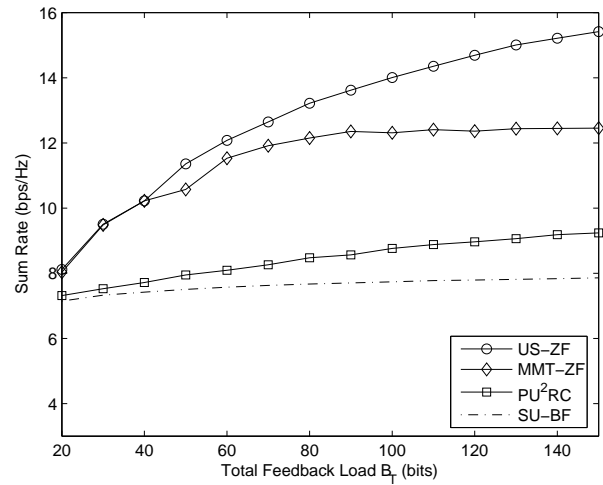
(a) Sum rates of different systems, $T = 100$ (b) Sum rates for different B_T , SNR=15 dB.

Fig. 8. Sum rates of different systems with a feedback overhead constraint. The curve of MMT-ZF is not smooth for different B_T due to the roundoff of $\lfloor \frac{B_T}{M} \rfloor$.